University of Arkansas, Fayetteville
ScholarWorks@UARK

Graduate Theses and Dissertations

8-2023

Rice Material State Diagrams: Trends of Contemporary Cultivars and Influence of Nitrogen Application During Production

Evans Ameyaw Owusu
University of Arkansas-Fayetteville

Follow this and additional works at: https://scholarworks.uark.edu/etd

Part of the Agriculture Commons, and the Food Science Commons

Citation

Ameyaw Owusu, E. (2023). Rice Material State Diagrams: Trends of Contemporary Cultivars and Influence of Nitrogen Application During Production. *Graduate Theses and Dissertations* Retrieved from https://scholarworks.uark.edu/etd/4882

This Thesis is brought to you for free and open access by ScholarWorks@UARK. It has been accepted for inclusion in Graduate Theses and Dissertations by an authorized administrator of ScholarWorks@UARK. For more information, please contact scholar@uark.edu.

Rice Material State Diagrams: Trends of Contemporary Cultivars and Influence of Nitrogen Application During Production

A thesis submitted in partial fulfillment
of the requirements for the degree of
Master of Science in Food Science

by

Evans Ameyaw Owusu
Kwame Nkrumah University of Science and Technology
Bachelor of Science in Food Science and Technology, 2018

August 2023
University of Arkansas

This thesis is approved for recommendation to the Graduate Council.

____

Griffiths G. Atungulu, PhD
Thesis Director

____

Ali Ubeyitogullari, PhD
Committee Member

____

Rusty Bautista, PhD
Committee Member

Abstract

Rice is typically harvested at high moisture content (MC) levels which necessitates drying to low MC levels for safe storage. However, drying at inappropriate temperatures and durations can lead to deterioration of kernel quality such as fissure formation. Kernels with these fissures are typically associated with reduced head rice yields and significant economic losses. Material state diagrams for rice have been created by the University of Arkansas Rice Processing Program (UARPP) as a tool to aid in predicting the ideal temperatures to use during drying and tempering (a process of holding rice at the drying temperature for some duration). The diagram is made up of the glass transition temperature (T_g) of rice at various MC levels. The T_g is used to define the boundary of the rice material's glassy and rubbery states and hence having accurate data on the T_g of rice is imperative to ensuring proper drying and tempering operations. Presently, the current rice material state diagrams were developed for old rice cultivars which may be inadequate for controlling the drying and tempering of the contemporary rice cultivars. Additionally, soil nitrogen application is stipulated to increase rice's amylose content, which tends to increase the T_g of rice starches. Therefore, the objective of this study was to generate material state diagrams for contemporary rice cultivars as well as determine the impact of soil Nitrogen on the T_g of a contemporary rice cultivar. The study involved conditioning samples of 23 rice cultivars harvested in 2022 to MC levels ranging from 20% to 12% as well as treating a long-grain pure-line cultivar (Diamond) with 6 different nitrogen rates (0, 100, 134, 168, 201, and 235 kg/ha) at the pre-flood stage. A differential scanning calorimeter was used to determine the T_g of these rice samples. The study revealed the average T_g of the rice samples to be 39, 41, 43, 45, and 47°C at MC levels of 20, 18, 16, 14, and 12%, respectively. Rice material state diagrams with these updated T_g were then developed. At a harvest MC of 20%, the brown rice in

this study exhibited a slightly higher T_g of approximately 39 °C compared to that of previous studies (approximately 36 °C), along with a better model accuracy of $R^2 = 0.72$. The study also revealed that the application of soil nitrogen at 100 and 168 kg/ha caused the T_g of the rice samples to significantly increase. Using this newly generated information, contemporary rice cultivars can be better controlled during drying and tempering.

Acknowledgment

Firstly, I would like to express my heartfelt gratitude to the Almighty God for His unwavering grace and blessings throughout my educational journey. I extend my deepest appreciation to my supervisor and thesis director, Dr. Griffiths Atungulu, for his trust in me and his exceptional guidance and mentorship given throughout this period.

I am immensely thankful to my committee members, Dr. Ali Ubeyitogullari, and Dr. Rusty Bautista for their constant encouragement, guidance, and mentorship during this program. I am truly grateful for the knowledge you shared with me, which has prepared me for the next chapter of my journey.

I would also like to extend my sincere appreciation to the University of Arkansas Division of Agriculture and the University of Arkansas Rice Processing Program for providing research facilities, support, and collaborations. I am also indebted to Dr. Ya-Jane Wang and Ana Gonzalez of the Department of food science, University of Arkansas, for their crucial assistance in conducting my laboratory analysis.

In addition, I wish to thank Dr. Kaushik Luthra, Robin January, Justin W. Siebenmorgen, Abass Adekoyejo Oduola, Samuel Olaoni, Faith Ouma, Devisree Chukkapalli, and Bindu Regonda from my research group. Your help with the technical aspects, love, and concern was crucial to this accomplishment.

I would also like to express my sincerest appreciation to my parents for their countless sacrifices and ongoing support. Finally, I am grateful for the unwavering support of my extended family, friends, and loved ones, who have brought out the best in me. Thank you all for standing by me always.

Table of Contents

List of Published Paper

Chapter II: Ameyaw Owusu, E., Luthra, K., & Atungulu, G. G. (2023). Rice Material State Diagrams: Trends of Contemporary Cultivars and Influence of Nitrogen Application During Production. *Journal of Cereal Chemistry*, (Submitted)

I. INTRODUCTION

In the US, rice is typically harvested at high moisture content levels between 16–21% wet-basis (w.b) and dried to approximately 12% for safe storage. Improper drying process can however lead to defects in the kernel structure, such as the formation of fissures. A rice material state diagram is a tool that can help predict the appropriate drying and tempering temperatures to employ during the drying of rice kernels. These diagrams consist of rice's glass transition temperature (T_g) at various moisture content levels. The present rice material state diagrams used are however developed for some old rice cultivars (Bengal, Cypress, and Drew) harvested between 1997 to 1999. These diagrams may hence be insufficient for describing the drying behaviors of contemporary pure-line and hybrid rice cultivars.

Additionally, soil nitrogen fertilizer application commonly employed for rice cultivation causes the synthesis of amylose, amylopectin, and their chain length in rice (Zhou et al., 2020). These changes are expected to affect the glass transition temperatures (T_g) of rice kernels during active drying which is critical in predicting the fissuring potential of rice kernels.

The objectives of this study were therefore, to generate material state diagrams with updated T_g for contemporary pure-line and hybrid rice cultivars as well as determine the role of soil nitrogen application on glass transition temperatures (T_g) of a selected newer long-grain rice cultivar.

II. RICE MATERIAL STATE DIAGRAMS: TRENDS OF CONTEMPORARY CULTIVARS AND INFLUENCE OF NITROGEN APPLICATION DURING PRODUCTION

A. ABSTRACT

Improper drying of rice can cause defects in the kernel such as fissuring that leads to reduced head rice yield and significant economic losses. The University of Arkansas Rice Processing Program has developed material state diagrams for rice, as a tool to help predict the appropriate drying and tempering temperatures to employ. These diagrams consist of the glass transition temperature (T_g) of rice at various moisture content levels. The industry presently employs rice material state diagrams developed for old rice cultivars which may be inadequate for controlling the drying and tempering of recently developed cultivars. Additionally, soil nitrogen application is stipulated to increase rice's amylose content, which tends to increase the T_g of rice starches. Therefore, the objectives of this study were (1) to generate material state diagrams for contemporary rice cultivars and (2) to determine the impact of soil nitrogen application on the T_g of a selected contemporary rice cultivar. The study involved conditioning samples of 23 rice cultivars harvested in 2022 to moisture content levels ranging from 20% to 12% for Objective 1. For Objective 2, a long-grain pure-line cultivar (Diamond) was treated with 6 different nitrogen rates (0, 100, 134, 168, 201, and 235 kg/ha) at the pre-flood stage. A differential scanning calorimeter was used to determine the T_g of these rice samples. The study found that the average T_g of the rice samples were 39, 41, 43, 45, and 47°C at MC levels of 20, 18, 16, 14, and 12%, respectively. Rice material state diagrams with these updated T_g were then developed. The study also revealed that the application of soil nitrogen at 100 and 168 kg/ha

caused the T_g of the rice samples to significantly increase. This newly generated information will help in better controlling the drying and tempering of contemporary rice cultivars.

Keywords: Glass Transition Temperature, Material State Diagrams, Nitrogen, Rice

B. INTRODUCTION

Material state diagrams are visual representations that depict the physical and chemical states of certain amorphous materials such as polymers, glass, and rubber, under different conditions. The physical states of a biopolymer material determine the transport properties such as viscosity, density, mass, and thermal diffusivity and reactivity of the material. Factors like temperature, moisture content, pressure, concentration, and time can alter these physical states of biopolymers. Two major biopolymers that can exist in an amorphous, metastable state and are sensitive to moisture and temperature changes are proteins and starches, which are present in varying amounts in a wide range of food products (Icoz and Kokini, 2008). The relationship between the composition and the physical states of such food products can be represented on a state diagram which can enable the understanding of the processing requirements as well as storage stability. These material state diagrams can predict the behavior of food biopolymers during baking, extrusion, and storage (Levine and Slade, 1990). According to Icoz and Kokini (2008), the most basic state diagrams for food systems are those formed by glass transition temperature as a function of moisture content. The glass transition temperature (T_g) is an important parameter that represents the temperature range where polymeric materials such as rice starches change from a hard glassy phase to a soft rubbery phase. This concept has been applied to identify the role of intra-kernel material state differences in rice kernels (Cnossen and Siebenmorgen, 2000).

Rice is a major commercial crop in the United States and one of the world's most essential staple foods. Rice is typically harvested at high moisture levels, which promotes the growth of spoilage microorganisms, and hence necessitates further drying to be stored safely (Mossman and Miller 1986). In the US, rice is typically harvested between 16–21% moisture content (MC) (w.b) and dried to approximately 12% MC for safe storage. According to multiple reports, improper drying activities can however lead to defects in the kernel structure (Kunze, 1979, Kunze and Prasad 1978, Sharma and Kunze 1982). Rice is largely composed of starch and is considered a biomaterial that is highly hygroscopic. During drying, the rice kernel undergoes a glass transition as the kernel goes through temperature and moisture content changes. Therefore, rice material state diagrams can be developed to better manage and improve the drying conditions used for rice kernels. Rice material state diagrams using the glass transition temperature concept have been used to explain rice fissure formation during drying (Cnossen and Siebenmorgen, 2000).

Rice kernels with internal fractures within the endosperm are commonly referred to as fissured kernels. It is the fissured kernels that usually break during milling, leading to significant reductions in milling yields. The functional properties of fissured rice kernels are also immensely affected after their milling (Siebenmorgen et al., 2005; Mukhopadhyay and Siebenmorgen, 2017). This leads to significant economic losses for end-use processors (Siebenmorgen et al., 2009). It is therefore imperative to minimize kernel fissuring formation in the rice industry, by understanding how these fissures tend to occur during the active drying of rice. Fissuring caused by improper drying of kernels is stipulated to be a result of material state differences between the kernel periphery (outer region) and the inner core, resulting in intra-kernel differential stresses (Cnossen and Siebenmorgen, 2000). This intra-kernel material state gradient results from temperature and moisture content (MC) differences within individual rice kernels that are generated while drying (Slade and Levin, 1995; Perdon et al., 2000).

According to the glass transition hypothesis using rice material state diagrams, fissuring of rice kernels can occur in two scenarios during drying (Cnossen and Siebenmorgen, 2000). The first hypothesis is displayed in Figure 1. The concept stipulates that as the temperature of the rice kernel approaches the drying air temperature during high-temperature drying, the condition of the grain changes from a glassy to a rubbery state. Over time, the surface layers of the kernel lose moisture at a more rapid rate than the core of the kernel. In this instance, the surface layers with lower moisture content due to the drying may transition back to the glassy state. This phenomenon proposes that in situations when drying is made longer such that ample portions of the kernel periphery (Fig. 1; point S) transition to a glassy state while the core (Fig. 1; point C) remains in a rubbery state, extreme conditions of intra-kernel material state gradients occur between the surface and the core areas. This, therefore, results in stresses which can exceed the kernel material strength, causing fissures to start occurring.

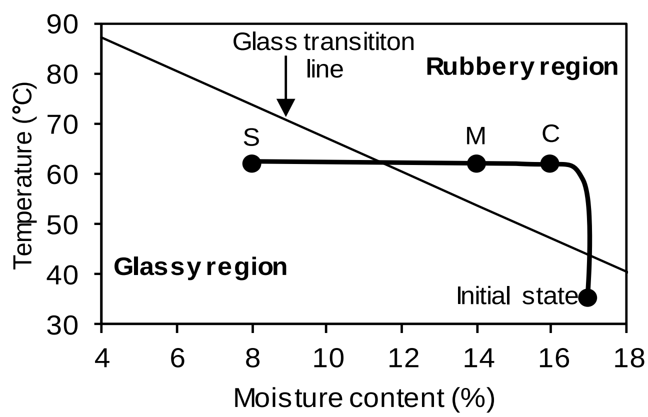

Figure 1. A hypothetical path of a rice kernel during prolonged high-temperature and low-relative humidity drying. Surface (S), midpoint (M), and center (C) correspond to locations within a rice kernel (Cnossen and Siebenmorgen, 2000).

The second scenario where fissuring is hypothesized to occur is when cooling is done right after drying without sufficient tempering (a process of holding rice at the drying temperature for some duration). This is due to the fact that although intra-kernel material state and MC gradients are generated during active drying, they might not be sufficient to result in fissuring. However, if these existing gradients after drying are not allowed to subside and the kernel is immediately cooled, the kernel surface and core will transition to the glassy state at different instances as shown in Figure 2 (point II). This as a result creates a more severe intra-kernel material state gradient that could cause fissuring.

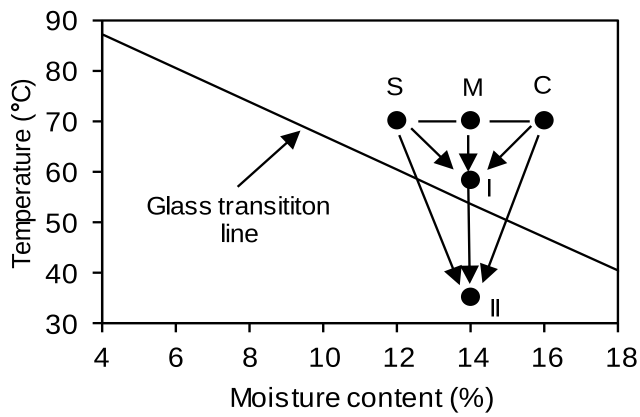

Figure 2. Hypothetical tempering situations above (I) and below (II) the glass transition temperature (T_g) for a rice kernel dried using air temperatures above T_g. Surface (S), midpoint (M), and center (C) correspond to locations within a rice kernel (Cnossen and Siebenmorgen, 2000).

The glass transition hypothesis indicates that when the tempering temperature is lower than the T_g of the rice, the kernel will undergo a state transition from rubbery into the glassy state as the kernel temperature decreases, resulting in kernel fissuring (Cnossen and Siebenmorgen, 2000). Data on the specific T_g of rice kernels can be very instrumental in developing material state diagrams that can predict the material states (glassy/rubbery) of rice kernels or portions of kernels at a given temperature and moisture content. The information provided by these material state diagrams can therefore inform the rice industry on the correct drying and tempering temperatures to employ for the safe drying of harvested rice kernels.

The current material state diagrams were however developed for old rice cultivars (Bengal, Cypress, and Drew) that were harvested between 1997 to 1999 (Perdon et al., 2000; Sun et al., 2002). These diagrams may be insufficient for describing the drying behaviors of contemporary pure-line and hybrid grain cultivars. This is because the properties of rice cultivars have significantly changed over the years with the introduction of more breeds. Intensive breeding conducted to enhance traits such as high yield and pest resistance have also resulted in changes to the rice genome. As such, different breeds of contemporary rice may have distinct properties such as starch compositions, size, shape, texture, and nutritional values (Sweeney & McCouch, 2007; Gross & Zhao, 2014). According to UAEX (2023), the best and most consistent cultivars in grain production and milling yield under a variety of environmental and management conditions include long grain pure-lines (DG263L, Ozark, Diamond, ProGold1, CLL16, CLL18), long grain hybrids (RT XP753, RT 7401, RT 7302, RT 7521 FP, RT 7321 FP, RT 7421 FP, RT 7331 MA, RTv7231 MA, PVL03), and medium grain varieties (Titan, Lynx, Jupiter, DG353M, CLM04). Due to the changing composition of physicochemical properties within these new cultivars, the development of new material state diagrams for these contemporary cultivars becomes essential.

Additionally, the application of nitrogen fertilizer on these contemporary rice cultivars has become a common practice. This is because Nitrogen is the most important element for plant growth, development, and quality, among all other nutrients. It is used extensively to increase rice crop yield by farmers because it improves crop performance, promotes plant leaf area, plant biomass, and finally crop yield (Sinclair, 1989). According to Zhou et al. (2020), nitrogen application affects the structure of rice starches, and as a result, changes the functional properties and the final quality of rice cultivars. The rice grain quality in terms of starch particle size, crystal structure, chain length distribution, and pasting properties are also immensely affected by nitrogen application on rice plants (Singh et al., 2011; Gu et al., 2015; Zhu et al., 2017; Zhang et al., 2019).

The impact of nitrogen fertilizer on rice grain quality is a result of its effects on carbohydrate biosynthetic enzyme activity. The biosynthesis of amylose is usually controlled by ADP glucose pyrophosphorylase (AGPase) and granule-bound starch synthase (GBSS). Biosynthesis of amylopectin on the other hand requires a coordinated series of enzymatic reactions that involve AGPase, soluble starch synthase (SS), starch branching enzyme (BE), and starch debranching enzyme (DBE), making it more complex. These syntheses of amylose, amylopectin, and the distribution of amylopectin chain-length (CLDs) tend to influence the textural attributes of rice (Zhou et al., 2020). Hence, soil nitrogen fertilizer application influences the synthesis of amylose, amylopectin, and their chain length in rice and these properties of the starches determine the physicochemical attributes of rice. Significant changes are caused in the physicochemical properties of rice due to nitrogen application. These changes tend to affect the glass transitions (T_g) of rice kernels during active drying which is critical in predicting the fissuring potential of rice kernels. A report by Liu et al. (2010), indicates that T_g increases with increasing amylose content, however, the influence of nitrogen application on the T_g of rice is unknown.

The objectives of this study were therefore, (1) to generate material state diagrams with updated T_g for contemporary pure-line and hybrid rice cultivars (2) to determine the role of soil nitrogen application on glass transition temperatures (T_g) of a selected newer long-grain rice cultivar.

C. MATERIALS AND METHODS

Sample Procurement and Preparation

In 2022, 23 different rough rice cultivars of high moisture contents (22 – 16%) wet basis (w.b) were harvested from rice plots in Harrisburg, Arkansas. 21 of these cultivars were sampled from two distinct plots making up 44 samples in total for objective 1. A long-grain pure-line cultivar (Diamond) treated with 6 different nitrogen rates applied was also obtained from the rice research and extension center, in Stuttgart, Arkansas. The nitrogen rates were applied at the pre-flood stage in kg/ha to obtain samples at 0, 100, 134, 168, 201, and 235 kg/ha for objective 2. The rough rice samples were cleaned using a dockage tester (XT4, Carter-Day, Minneapolis, USA). A precision sizer (ABF2, Carter-Day Company, Minneapolis, MN) was used to grade the thickness of the rough rice samples to achieve uniformity in kernels and reduce variation in samples used during the experiment. A thickness size of 1.88 - 1.98 mm was used to screen long-grain cultivars while a thickness size of >2.03 mm was used to screen medium-grain cultivars. This ensured that all immature kernels were removed from the rice samples. The cleaned and size fractioned rough rice samples were conditioned to 12% moisture content (w.b) using natural air drying and an equilibrium moisture content (EMC) chamber set at 25°C and 56% relative humidity. During the drying process, the moisture contents of the rough rice samples were measured to obtain samples of 20%, 18%, 16%, 14%, and 12% (w.b). This was achieved by measuring the MC of the samples in triplicates using the moisture content meter (AM 5200–A, PerkinElmer, Hagersten, Sweden). Samples of brown rice were obtained by hand de-hulling the hulls from each of the rough rice samples. The dimensions of the brown rice samples for each cultivar were measured in duplicates using the Seed Count (A7050, Stadvis Pty Ltd, Australia). The samples of brown rice obtained at various MC levels were then kept in sealed plastic tubes and stored at 4 °C before further analysis. Figures 3 and 4 are flowcharts that describe the methodology employed for objectives 1 and 2 respectively.

Differential Scanning Calorimetry Analysis

The glass transition temperatures of samples at various MC levels were determined using a differential scanning calorimeter (Diamond DSC, Perkin Elmer, Shelton, CT). The DSC equipment measures the amount of energy (heat) absorbed or released by a sample as it is heated, cooled, or held at a constant (isothermal) temperature. Multiple thermal properties of a sample including T_g, gelatinization temperature, melting temperature, specific heat, crystallization temperature, oxidative induction time, and % cure can be obtained using the DSC.

The DSC analysis was conducted according to the methodology by Perdon et al. (2000), with few modifications. In the analysis, each brown rice kernel was cross-sectioned into two parts using a razor blade. The sectioned kernels were placed in a pre-weighed high-pressure stainless-steel pan and sealed. The sealed pan was then weighed to obtain the weight of the sample. A sealed empty high-pressure stainless-steel pan was used as the reference. The DSC system was then set to equilibrate the sectioned brown rice samples to –30°C and then heated from –30 to 250°C at a rate of 5°C/min. The T_g from each thermogram was then determined by identifying the transition corresponding to a slope change in the heat capacity of the sample where the glass transition occurs.

Statistical Analyses

The study was conducted as a completely randomized design. A Simple linear regression model was fitted from the experimental data, using JMP Pro 17 statistical software (JMP Pro 17, SAS Institute, Cary, NC). Tukey's HSD test was employed to compare the means and the level of significance was set at a 95% confidence level.

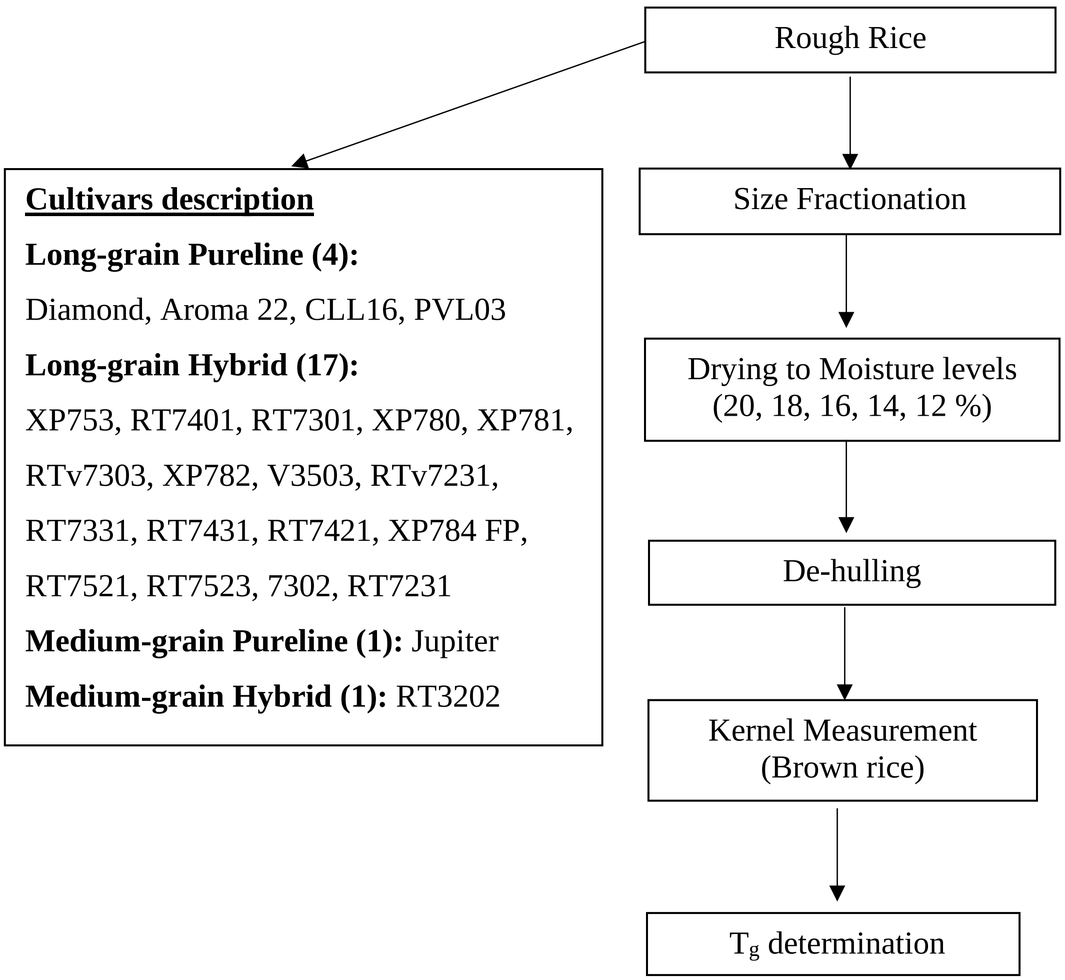

Figure 3. Flow diagram outlining methodology for objective 1.

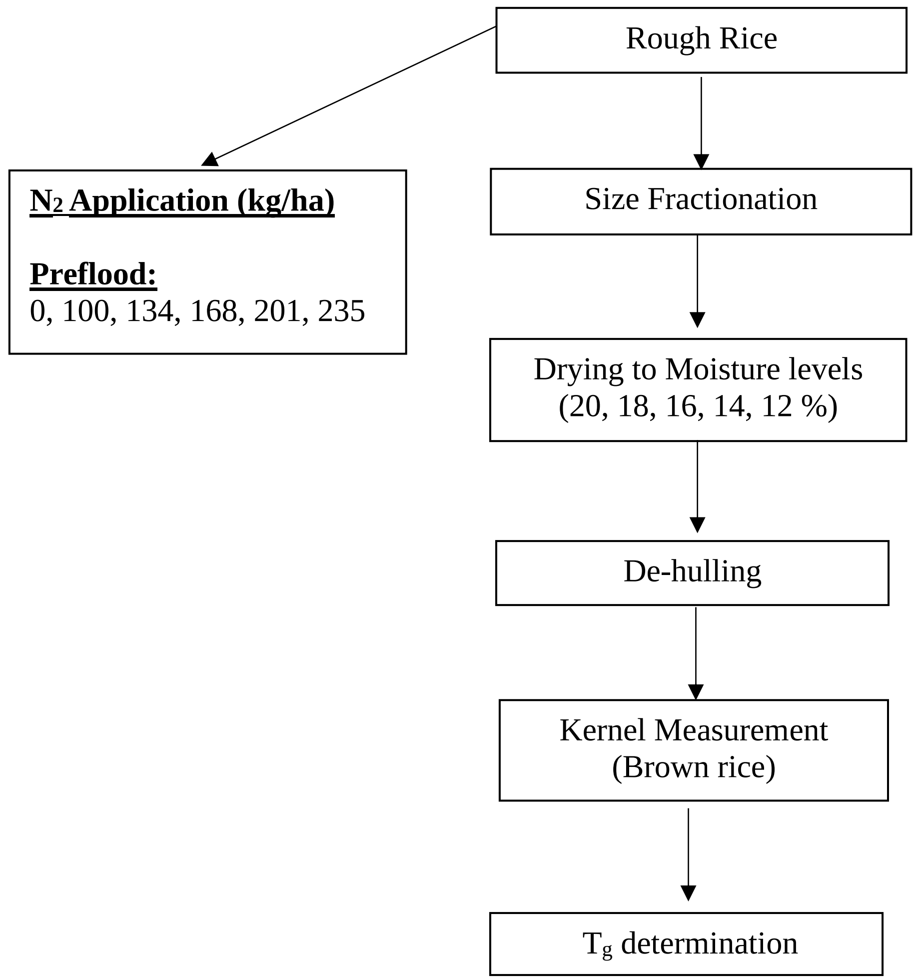

Figure 4. Flow diagram outlining methodology for objective 2.

D. RESULTS AND DISCUSSION

Kernel Dimensions Measurement

The kernel dimensions (length, width, thickness) of each cultivar experimented on are presented in Table 1 for the long-grains and Table 2 for the medium-grain cultivars. For the long-grain cultivars, the average length, width, and thickness of the kernels were 7.15 ± 0.19 mm, 2.24 ± 0.08 mm, and 1.79 ± 0.04 mm, respectively. And for the medium-grain cultivars, the average length, width, and thickness of the kernels were 6.05 ± 0.17 mm, 2.75 ± 0.05 mm, and 2.14 ± 0.05 mm respectively. The dimensions of these contemporary rice cultivars were slightly higher compared to some old cultivars (Bengal, Cypress) explored in previous studies. The mean length, width, and thickness of Bengal (medium-grain cultivar) were 6.2 mm, 2.5 mm, and 1.9 mm respectively while the mean length, width, and thickness of Cypress (long-grain cultivar) was 6.8 mm, 2.2 mm, and 1.8 mm respectively (Perdon et al., 2000). These differences in dimensions could be indicative of reports that suggest a significant increase in kernel sizes over the years (Takano-Kai et al., 2009).

Table 1.0 Kernel dimensions of long-grain brown rice cultivars

Cultivar	**Length (mm)**	**Width (mm)**	**Thickness (mm)**
RT7401 1	6.91	2.16	1.78
RT7301 1	6.91	2.3	1.8
XP753 1	6.99	2.2	1.75
XP780 1	7.31	2.33	1.81
7302	7.24	2.2	1.8
XP781 1	7.2	2.34	1.81
RTV7303 1	7.17	2.1	1.79
XP782 1	7.22	2.35	1.83
V3503 1	7.21	2.11	1.89
DIAM 1	7.1	2.24	1.78
XP753 2	6.96	2.24	1.77
RT7401 2	6.89	2.16	1.77
RT7301 2	6.91	2.3	1.75
XP780 2	7.29	2.31	1.76
XP781 2	7.26	2.32	1.8
RTV7303 2	7.03	2.17	1.81
XP782 2	7.14	2.34	1.8
DIAM 2	7.15	2.28	1.79
V3503 2	7.24	2.14	1.77
RT7321 1	7.02	2.26	1.79
RT7421 1	7.03	2.23	1.76
XP784 1	7.33	2.17	1.84
RT7521 1	7.11	2.28	1.79
RT7523 1	7	2.25	1.79
CLL16 1	7.53	2.39	1.85

RT7321 2	7.22	2.29	1.79
RT7421 2	7.07	2.26	1.77
XP784 2	7.38	2.15	1.88
RT7521 2	7.17	2.38	1.78
RT7523 2	7.14	2.24	1.78
CLL16 2	7.46	2.28	1.85
PVL03 1	7.59	2.23	1.87
RT7231 1	6.98	2.08	1.75
RT7331 1	7.02	2.25	1.73
RT7431 1	7.04	2.37	1.82
PVL03 2	7.52	2.27	1.85
RT7231 2	6.91	1.98	1.79
RT7331 2	7.06	2.28	1.75
RT7431 2	6.86	2.17	1.73
Aroma 22	7.49	2.24	1.77

"1" and "2" correspond to the cultivars grown in plots 1 and 2, respectively.

Table 2.0 Kernel dimensions of medium-grain brown rice cultivars

Cultivar	**Length (mm)**	**Width (mm)**	**Thickness (mm)**
Jupiter 1	6.05	2.73	2.22
RT3202 1	6.08	2.74	2.13
Jupiter 2	6.06	2.82	2.11
RT3202 2	6.04	2.71	2.12

"1" and "2" correspond to the cultivars grown in plots 1 and 2, respectively.

Measurement of T_g using Differential Scanning Calorimetry

From the data obtained from the DSC analysis, three major transitions—a low-temperature transition, an intermediate-temperature transition, and a high-temperature transition—were observed in the brown rice kernels between 0 and 250°C. This was similar to trends observed in studies by Perdon et al. (2000) and Sun et al. (2002). According to Perdon et al. (2000), the T_g of rice kernels was assumed to be the transition at low temperatures, whereas the intermediate temperature transition was hypothesized to be related to the rapid evaporation of moisture from the rice kernels. The high-temperature transition was related to the point where the melting of the crystalline starch of the rice kernels occurred. The T_g of the contemporary rice cultivars at the various MC levels were therefore taken from the low-temperature transitions. The approximate temperatures within this low-temperature transition ranged from 39°C to 47°C. Specifically, the T_g of the rice samples was approximately 39, 41, 43, 45, and 47°C at MC levels of 20, 18, 16, 14, and 12%, respectively. Rice material state diagrams with these updated T_g were then developed for contemporary cultivars.

Development of Rice Material State Diagrams

Material state diagrams were generated for the different rice cultivars, by plotting their T_g against their respective MC (12–20%). From the material state diagrams, a strong negatively correlated linear relationship existed between the MC and the T_g. The T_g of the rice kernels increased with decreasing moisture content. This was similar to trends observed in studies by Perdon et al. (2000) and Sun et al. (2002). The account for this relationship indicates that water (moisture content) had a significant effect on the T_g. of rice kernels. An additional factor that accounts for this relationship is the effect of molecular weight (MW) distribution of the starch. The relationship of T_g. to MW is well established as an increase in MW will typically correlate with increased T_g. (Slade and Levine 1991). This is due to the fact that rice harvested at high MC levels frequently have immature kernels, which may have lower MW starch due to incomplete starch synthesis. Drying rice kernels to lower MC levels will therefore lead to an increase in MW starch which correlates with increased T_g. (Slade and Levine 1995; Perdon et al., 2000).

Figures 5, 6, 7, and 8 show material state diagrams for medium-grain pure-line, medium-grain hybrid, long-grain pure-line, and long-grain hybrids. The material state diagram for all contemporary rice cultivars explored in this study is shown in Figure 9. As shown by the regression functions of the figures, the T_g values of the medium-grain hybrid cultivar (RT3202) were slightly higher than that of the medium-grain pure-line cultivar (Jupiter) but were not statistically different ($P \leq 0.05$). Additionally, the long-grain pure lines (Fig.7) had slightly higher T_g values than the long-grain hybrid cultivars (Fig.8) but were not significantly different ($P \leq 0.05$). The T_g values of the medium grain cultivars from the study were however significantly higher compared to the long grain cultivars ($P \leq 0.05$). The T_g vs MC relationship obtained from the contemporary rice cultivars (long-grain pure lines, long-grain hybrids, medium-grain pure lines, and medium hybrids) explored in this study (Fig. 9) can be represented by a regression function as in equation 1.

$$T_g = 59.12 - 1.02\ MC, \quad R^2 = 0.72 \qquad (1)$$

From previous studies, the T_g vs MC relationship for (Bengal and Cypress) cultivars by Perdon et al. (2000) is represented by equation 2, whereas the relationship for the Drew cultivar by Sun et al. (2002) is represented by equation 3.

$$T_g = 57.03 - 1.08\ MC, \quad R^2 = 0.53 \qquad (2)$$

$$T_g = 59.47 - 1.17\ MC, \quad R^2 = 0.57 \qquad (3)$$

The T_g values obtained from the contemporary cultivars explored in the study were higher compared to that from the previous studies. At a typical harvest MC of 20%, the T_g of brown rice from this study is approximately 39 °C, which is slightly higher compared to that of the previous studies at approximately 36 °C. There was also a higher R^2 value, explaining about 72% of variations in the new model. The results from this study, therefore, recommend drying and tempering rice cultivars presently used at temperatures above the glass transition line (Fig.9). This will help prevent the rice material from undergoing a further glass transition into the glassy state as the kernel temperature decreases, which can ultimately lead to defects such as kernel fissuring (Cnossen and Siebenmorgen, 2000).

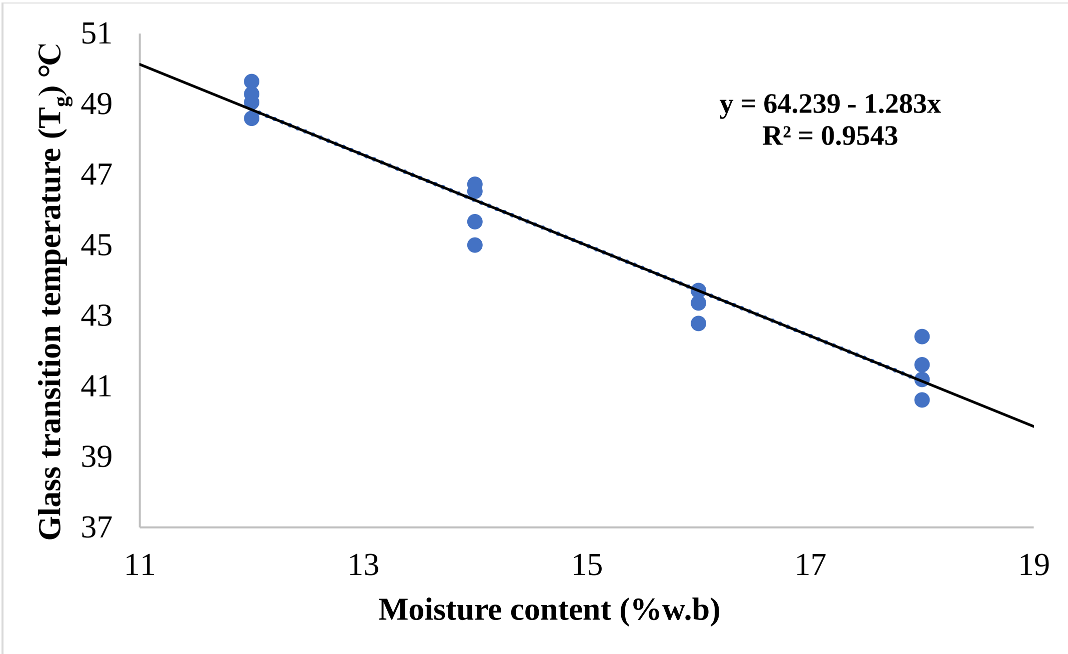

Figure 5. Material state diagram for medium-grain pure-line rice (Jupiter).

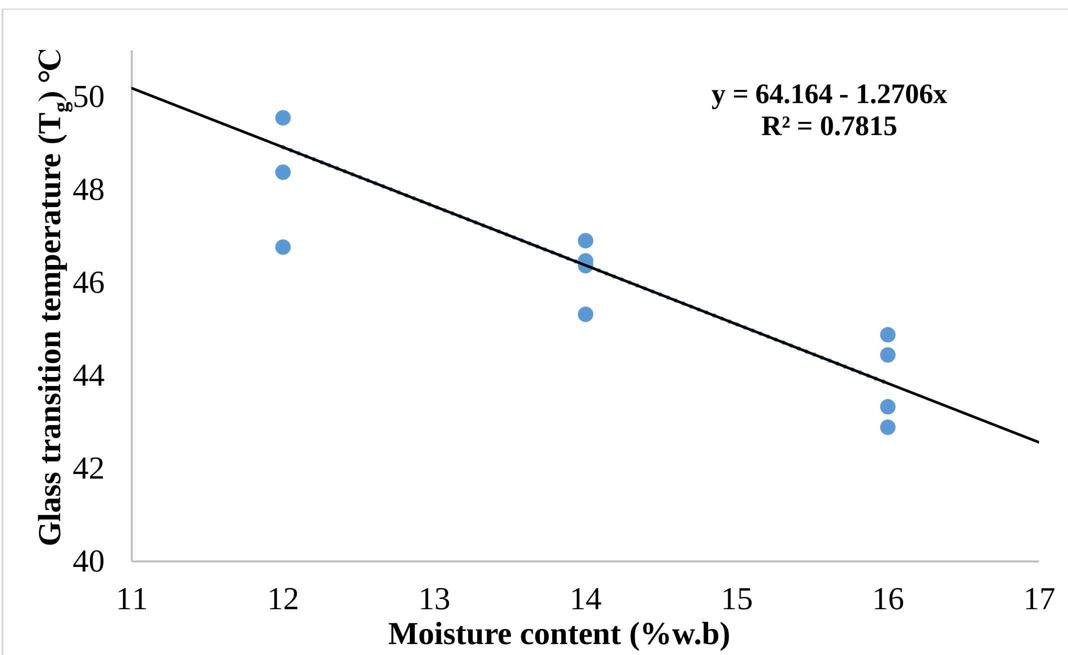

Figure 6. Material state diagram for medium-grain hybrid rice (RT3202).

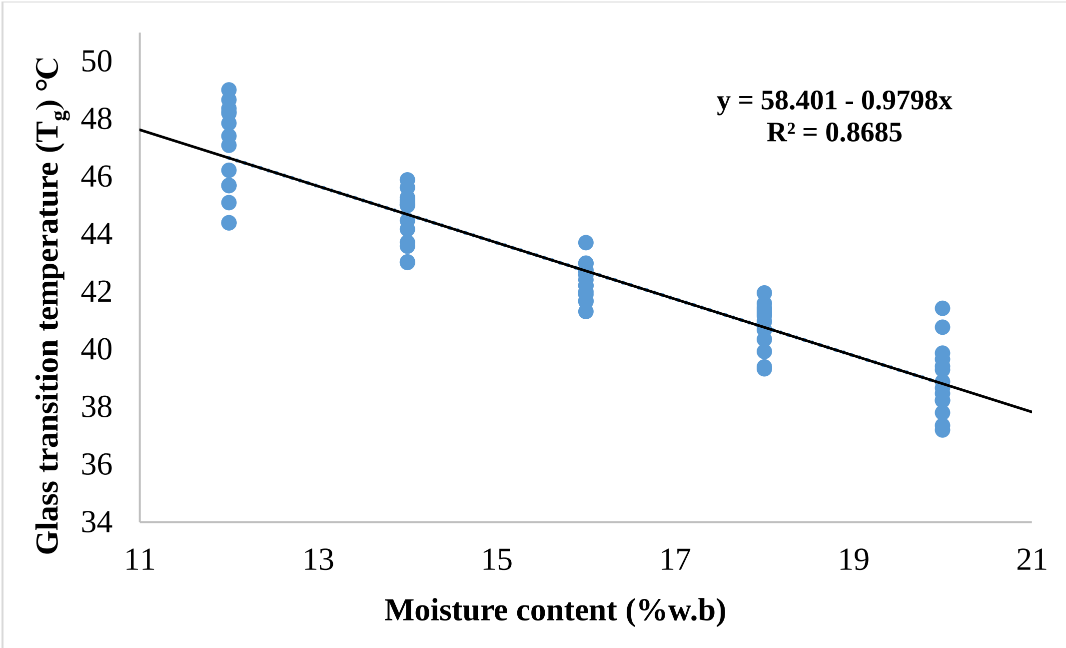

Figure 7. Combined material state diagram for long-grain pure-line rice (Diamond, Aroma 22, CLL16, PVL03)

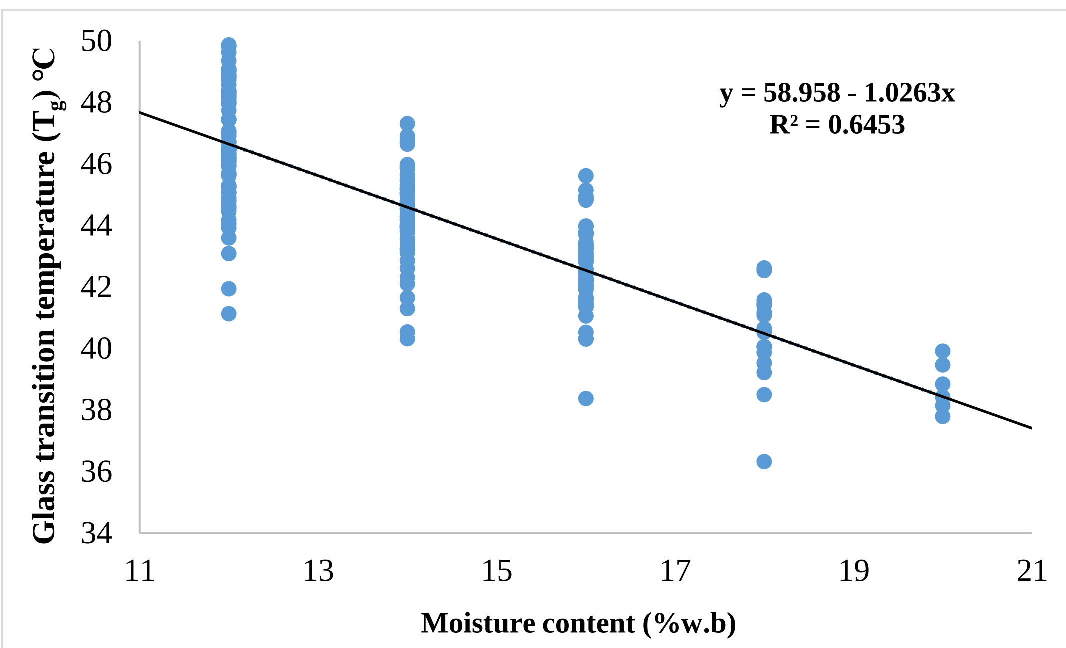

Figure 8. Combined material state diagram for long-grain hybrid rice (XP753, RT7401, RT7301, XP780, XP781, RTv7303, XP782, V3503, RTv7231, RT7331, RT7431, RT7421, XP784 FP, RT7521, RT7523, 7302, RT7231).

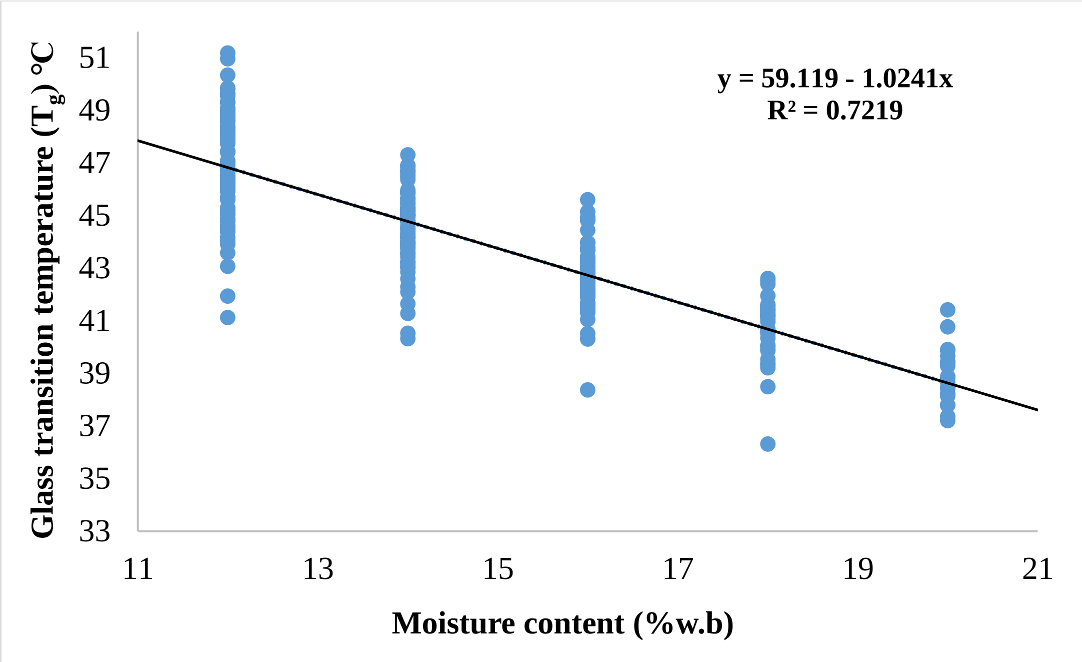

Figure 9. Combined material state diagram for contemporary rice (Jupiter, RT3202, Diamond, Aroma 22, CLL16, PVL03, XP753, RT7401, RT7301, XP780, XP781, RTv7303, XP782, V3503, RTv7231, RT7331, RT7431, RT7421, XP784 FP, RT7521, RT7523, 7302, RT7231).

Nitrogen Application on T_g of Rice

The glass transition temperatures of the various nitrogen-treated samples were also analyzed and presented in Table 3. The results indicated that the different samples explored as well as the various MC levels had significant effects ($\alpha = 0.05$) on the glass transition temperatures. Fig 10. shows the effects the various nitrogen-treated samples had on the glass transition temperatures. The results indicated that the sample with no nitrogen treatment (0 kg/ha) had the lowest mean T_g compared to the samples with nitrogen treatment. Treated samples at 100 and 168 kg/ha were however significantly higher compared to the control sample (0 kg/ha). This could be support for the theory that T_g rises with increasing amylose content, suggesting that the Nitrogen may have elevated amylose levels in the rice samples.

Table 3. Statistical analysis of the effects of Sample and MC on T_g

Source	P - value
Sample	0.0066*
MC	< 0.001*

(*) Indicate statistical significance at $\alpha = 0.05$

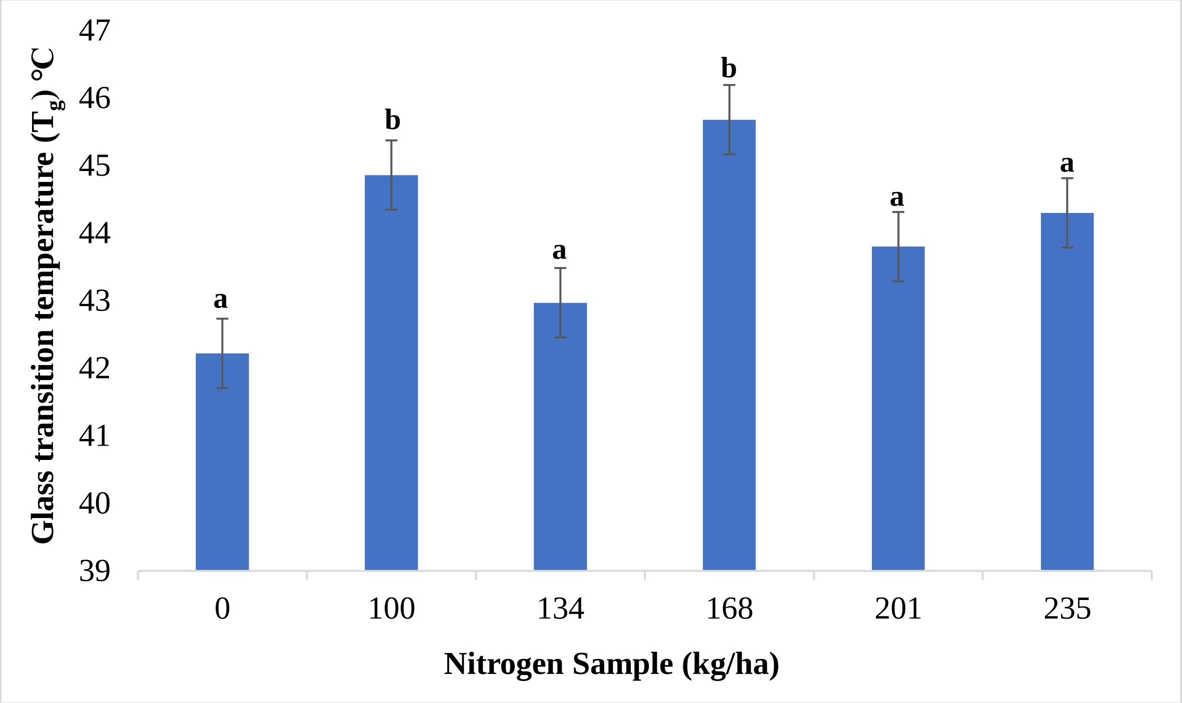

Figure 10. Mean Tg at various Nitrogen treated samples.
Different letters indicate significant difference at $\alpha = 0.05$

E. CONCLUSIONS

Rice material state diagrams with updated T_g were developed for the contemporary rice cultivars explored. The average T_g of the rice samples were 39, 41, 43, 45, and 47°C at MC levels of 20, 18, 16, 14, and 12%, respectively. The T_g of the brown rice in this study were slightly higher (approximately 39 °C at 20%) compared to that of previous studies (approximately 36 °C at 20%), along with a better model accuracy of $R^2 = 0.72$. Additionally, the application of soil N_2 caused a significant increase in the T_g of rice samples treated at 100 and 168 kg/ha. Further studies need to be carried out to investigate how applying nitrogen at different rates, timings and locations will impact the glass transition (T_g**)** of rice samples of different cultivars.

F. ACKNOWLEDGMENTS

Arkansas Rice Processing Program and the University of Arkansas System Division of Agriculture are immensely appreciated for their support and facilities. Special thanks to RiceTec for sample acquisition, Dr. Ya-Jane Wang of the Food Science Department, and all members of Dr. Griffiths Atungulu's lab for their kind guidance and service in this research.

G. REFERENCES

Cnossen, A. G., & Siebenmorgen, T. J. (2000). The glass transition temperature concept in rice drying and tempering: Effect on milling quality. *Transactions of the ASAE*, *43*(6), 1661.

Gross, B. L., & Zhao, Z. (2014). Archaeological and genetic insights into the origins of domesticated rice. *Proceedings of the National Academy of Sciences*, *111*(17), 6190-6197.

Gu, J. F., Chen, J., Chen, L., Wang, Z. Q., Zhang, H., & Yang, J. C. (2015). Grain quality changes and responses to nitrogen fertilizer of japonica rice cultivars released in the Yangtze River Basin from the 1950s to 2000s. Crop Journal, 4, 285-297.

Icoz, D. Z., & Kokini, J. L. (2008). State diagrams of food materials. *Food Materials Science: Principles and Practice*, 95-121.

Kunze, O. R. 1979. Fissuring of the rice grain after heated air drying. *Trans. ASAE* 22:1197-1202, 1207.

Kunze, O. R., and Prasad, S. (1978). Grain fissuring potentials in harvesting and drying of rice. *Trans. ASAE* 21:361-366.

Levine, H., & Slade, L. (1990). Influences of the glassy and rubbery states on the thermal, mechanical, and structural properties of doughs and baked products. *Dough rheology and baked product texture*, 157-330.

Liu, P., Yu, L., Wang, X., Li, D., Chen, L., & Li, X. (2010). Glass transition temperature of starches with different amylose/amylopectin ratios. *Journal of Cereal Science*, *51*(3), 388-391.

Mossman, A. P., & Miller, G. E. (1986). A review of basic concepts in rice-drying research. *Critical Reviews in Food Science & Nutrition*, *25*(1), 49-71.

Mukhopadhyay, S., & Siebenmorgen, T. J. (2017). Physical and functional characteristics of broken rice kernels caused by moisture-adsorption fissuring. *Cereal Chem.*, *94*(3), 539-545.

Perdon, A., Siebenmorgen, T., & Mauromoustakos, A. (2000). Glassy state transition and rice drying: Development of a brown rice state diagram. *Cereal Chem.*, *77*(6), 708-713.

Sharma, A. D., and Kunze, O. R. (1982). Post-drying fissure developments in rough rice. *Trans. ASAE* 25:465-468, 474.

Siebenmorgen, T., Qin, G., & Jia, C. (2005). Influence of drying on rice fissure formation rates and mechanical strength distributions. *Trans. ASAE*, *48*(5), 1835-1841.

Siebenmorgen, T., Saleh, M., & Bautista, R. (2009). Milled rice fissure formation kinetics. *Trans. ASABE*, *52*(3), 893-900.

Sinclair, T.R.; Horie, T. (1989). Leaf nitrogen, photosynthesis, and crop radiation use efficiency: A review. Crop Sci., 29, 90–98.

Singh, N., Pal, N., Mahajan, G., Singh, S., & Shevkani, K. (2011). Rice grain and starch properties: Effects of nitrogen fertilizer application. *Carbohydrate Polymers*, 86 219-225.

Slade, L., Levine, H., & Reid, D. S. (1991). Beyond water activity: recent advances based on an alternative approach to the assessment of food quality and safety. *Critical Reviews in Food Science & Nutrition*, 30(2-3), 115-360.

Slade, L., & Levine, H. (1995). Glass transitions and water-food structure interactions. *Advances in food and nutrition research*, 38, 103-269.

Sun, Z., Yang, W., Siebenmorgen, T., Stelwagen, A., & Cnossen, A. (2002). Thermomechanical transitions of rice kernels. *Cereal chemistry*, *79*(3), 349-353.

Sweeney, M., & McCouch, S. (2007). The complex history of the domestication of rice. *Annals of botany*, *100*(5), 951-957.

Takano-Kai, N., Jiang, H., Kubo, T., Sweeney, M., Matsumoto, T., Kanamori, H., ... & McCouch, S. (2009). Evolutionary history of GS3, a gene conferring grain length in rice. *Genetics*, *182*(4), 1323-1334.

Zhang, W., Yang, Q., Xia, M., Bai, W., Wang, P., Gao, X., Li, J., Feng, B., & Gao, J. (2019). Effects of nitrogen level on the physicochemical properties of Tartary buckwheat (Fagopyrum tataricum (L.) Gaertn.) starch. *International Journal of Biological Macromolecules*, 129: 799-808.

Zhou, T., Zhou, Q., Li, E., Yuan, L., Wang, W., Zhang, H. & Gu, J. (2020). Effects of nitrogen fertilizer on structure and physicochemical properties of ‘super’rice starch. *Carbohydrate polymers*, *239*, 116237.

Zhu, D., Zhang, H., Guo, B., Xu, K., Dai, Q., Wei, C., Zhou, G., & Huo, Z. (2017). Effects of nitrogen level on structure and physicochemical properties of rice starch. *Food Hydrocolloids*, 63, 525-532.

III. CONCLUSIONS

Rice material state diagrams consist of the T_g at various MCs of rice kernels and can help predict the appropriate temperatures to dry or temper rice kernels. From the study, the average updated T_g determined for contemporary rice cultivars were 39, 41, 43, 45, and 47°C at moisture content levels of 20, 18, 16, 14, and 12%, respectively. These T_g were slightly higher (approximately 39 °C at 20%) compared to that of previous studies (approximately 36 °C at 20%), along with a better model accuracy of $R^2 = 0.72$. These results can be used to predict the transition states (glassy/rubbery) of rice kernels at given temperatures and MCs. According to the study, using rice for drying and tempering at temperatures lower than the projected T_g (39 °C) at a typical harvest MC (20%) will probably cause a further transition of the kernel material state, which may result in the rice kernel fissuring. Additionally, the application of soil N_2 was found to cause a significant increase in the T_g of rice samples treated at 100 and 168 kg/ha. Therefore, further studies need to be carried out to investigate how applying nitrogen at different rates, timings and locations will impact the glass transition (T_g) of rice samples of different cultivars.